COBEM 2023 27TH INTERNATIONAL CONGRESS OF MECHANICAL ENGENEERING

ABCM Brazilian Society of Mechanical Sciences and Engineering
27th ABCM International Congress of Mechanical Engineering
December 04-08, 2023, Florianópolis-SC, Brazil

COB-2023-2156
MECHANICAL PROPERTIES OF POLYLACTIC ACID USED IN COMPONENTS MANUFACTURED IN 3D PRINTING

Luíza Guimarães de Albuquerque
Geice Paula Villibor
Universidade Federal de Viçosa, Av. Peter Henry Rolfs, s/n, Campus Universitário, 36570-900 Viçosa-MG
luiza.albuquerque@ufv.br
geice.villibor@ufv.br

Pedro Henrique de Moura Rodrigues
Universidade Federal de Viçosa, Av. Peter Henry Rolfs, s/n, Campus Universitário, 36570-900 Viçosa-MG
pedro.moura@ufv.br

Joseph Kalil Khoury Junior
Universidade Federal de Viçosa, Av. Peter Henry Rolfs, s/n, Campus Universitário, 36570-900 Viçosa-MG
kalil@ufv.br

Abstract. *The objective of this work was to study the influence of printing parameters on the mechanical properties of components made of polylactic acid (PLA). The printer used was the Ender brand, model 3. The dimensions of the specimen and tests procedure were defined based on ASTM D638. The printing parameters studied were two infill percentages (50 and 80%) and two printing speeds of the extruder nozzle (30 and 50 mm/s). Tensile tests were performed using an Instrom® test machine, model 3365, with a maximum capacity of 5 kN working with displacement speed of 5 mm/min. The parameters determined were modulus of elasticity and tensile strength. The significant influence of the interaction between printing speed and infill percentages on the determined modulus of elasticity was verified. For tensile strength the parameters printing speed and infill percentage influenced individually. The general average value found for the modulus of elasticity and tensile strength were 847.43 MPa and 35.95 MPa, respectively. The values obtained corroborate those determined by other authors in tests using the same material on different printers. Thus, by knowing the mechanical properties of PLA in 3D printing it is possible to design components with reduced mass, reliable and with greater durability.*

Keywords: *printing parameters, ASTM D638, Modulus of elasticity, Tensile strength*

1. INTRODUCTION

3D printing is widely used as an innovative technology for manufacturing mechanical components for several applications. Also known as additive manufacturing, is a revolutionary technique that allows the creation of three-dimensional objects layer by layer, based on digital modeling. Among some advantages of 3D printing, we can highlight the manufacture of objects with more complex shapes, the low waste and the possibility of recycling and reusing the material, the wide variety of materials that can be used as raw material and the greater ease customization and adaptation of the final product that can be used in the most diverse areas of the industry (Fico et al., 2022).

One of the most commonly used processes in 3D printing is Fused Filament Fabrication (FFF). FFF is an additive manufacturing technique that utilizes a thermoplastic filament as the feedstock material. During the process, the filament is heated until it reaches the melting point and then extruded through a computer-controlled extrusion nozzle to deposit the melted material in successive layers, forming the desired object (Gibson et al., 2015).

The use of low-cost 3D printing materials such as polylactic acid (PLA), acrylonitrile butadiene styrene (ABS), and polyethylene terephthalate glycol (PET-G) has gained attraction due to their versatility and affordability. These materials are being used to develop parts for vehicles such as drones and underwater vehicles, as well as to prototype face shields used during the COVID-19 pandemic. Among the most common filaments, polylactic acid (PLA) stands out. It is a biodegradable and biocompatible polymer derived from renewable resources such as corn starch and sugarcane. Ease of handling, low toxicity, sufficient strength, and good dimensional stability make it one of the most popular materials for 3D printing (Bellini et al., 2017).

However, the lack of complete and reliable information regarding the mechanical properties of these materials presents challenges for designers and engineers utilizing 3D printing. According to Souza et al. (2019), in most cases, there is incomplete information from manufacturers regarding the mechanical properties of materials used in 3D printers, and in some cases, this information is not available. This affects the reliability, safety, and durability of their designs.

Therefore, it is crucial to study and understand the influence of printing parameters on the mechanical properties of parts made from 3D printed materials. According to Smith et al. (2018), a detailed study of the mechanical properties of 3D printed materials is essential for the development of more reliable and durable projects. When printing objects using FFF technology, various printing parameters can be adjusted to optimize the quality and characteristics of the final part. These parameters include extrusion temperature, print speed, layer thickness, infill pattern type, and infill percentage. For example, Mensah et al. (2022) observed that the tensile strength and ductility improved significantly with increasing infill density, for 3D printed PLA parts .

In this context, the objective of this study is to investigate the influence of printing parameters on the mechanical properties of components fabricated using polylactic acid (PLA). PLA is one of the most commonly used materials in 3D printing due to its ease of processing and biodegradability. The effects of two fill levels (50.0%) and two extruder nozzle printing speeds (30 and 50 mm/s) on the tensile test results of PLA printed parts are investigated. Based on the obtained results, it will be possible to gain a better understanding of the mechanical properties of 3D printed PLA and design lighter, more reliable, and durable components. As reported by Johnson et al. (2020), the knowledge of the mechanical properties of 3D printed materials is crucial for the development of optimized and safe designs.

By filling this knowledge gap and providing official data on the mechanical properties of 3D printed PLA, this research will improve the use of this manufacturing technique and contribute to advanced advancements in component design and materials engineering. The objective of this research is to determine the mechanical properties of the PLA polymer after 3D printing through tensile testing.

2. MATERIAL AND METHODS

The chosen material for this study was PLA, as it is a commercially available material with good printability and cost-effectiveness among the options available. Therefore, the printing temperatures were kept consistent for all sample groups, as they depend on the material's melting point. A 1.75 mm diameter polymeric filament was evaluated for 3D Printing: Brand 1- PLA (white color). The material was characterized in its condition after being processed through the extrusion additive manufacturing technology.

Since parts produced by the FFF process have a mesostructure formed by void density and the presence of connections between deposited filaments within and between layers (Figure 3), the mesostructure determines the path of filament deposition and process parameters. The size and shape of voids and the extent of connection (contact area) between individual filaments are factors that influence the anisotropy of the parts and the value of mechanical strength (Rodriguez et al., 2000; Alaimo et al., 2017).

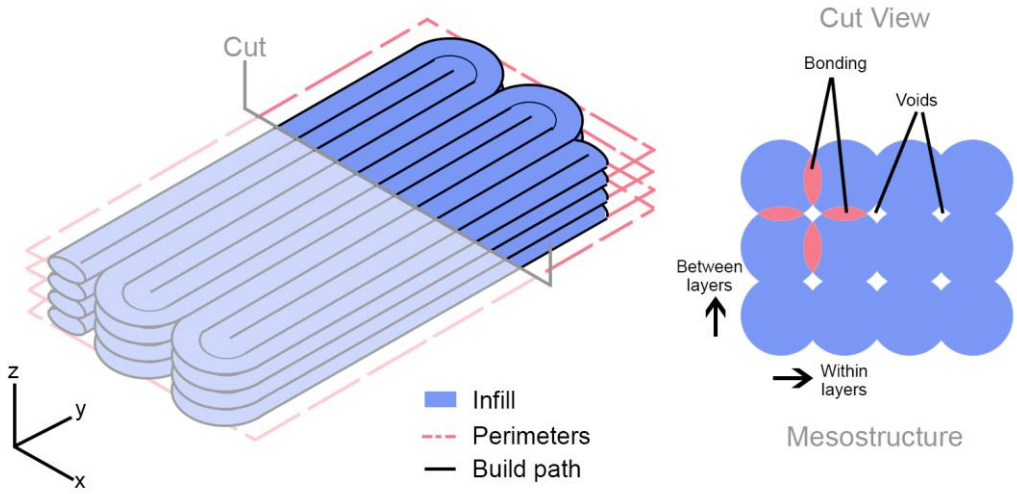

Figure 1. Representation of the mesostructure of parts manufactured by FFF (ADAPTED from: SANTANA, 2018).

Thus, based on the importance of printing parameters in the manufacturing process and determination of the mechanical properties, the test specimens for tensile testing were printed with geometries (Figure 2) and dimensions (Table 1). The test was based on ASTM D638 - Standard Test Methods for Tensile Properties of Plastics. Therefore, for this study, the A_{min} used, which will later be used as the nominal area for the tensile test, is 41.6 mm².

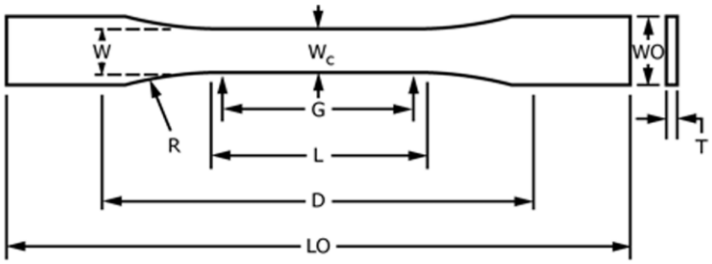

Figure 2. Geometry of Type 1 test specimen. Source: ASTM D638, 2014.

Table 1. Dimensions of Specimens, measured in mm (inches). Source: ASTM D638, 2014.

Dimensions (as per drawing)	**Measurements**	**Tolerances**
W – Width of narrow section	13 (0.50)	±0.50 (±0.02)
L – Length of narrow section	57 (2.25)	±0.50 (±0.02)
WO – Width overall	19 (0.75)	+6.40 (+0.25)
LO – Length overall	165 (6.50)	-
G-Gage Length	50 (2.00)	±0.25 (±0.01)
D – Distance between grips	115 (4.50)	±5 (±0.20)
R – Radius of fillet	76 (3.00)	±1 (±0.04)
T – Thickness	3.2 (0.13)	±0.40 (±0.02)

Among the printing parameters presented in the bibliographic references, only two were varied: extruder nozzle speed (NS) and infill percentage (IP), which, after combinations, generated sample groups with different configurations. The number of combinations generated by varying these parameters can be easily calculated by multiplication, as shown in Equation (1).

$$C = NS \times IP \tag{1}$$

The parameters that remained unchanged in the four configuration combinations were set as follows: layer thickness (LT) (0.2 mm), number of perimeters (NP) (3 perimeters), scanning angle (45°/-45°), build orientation (XY plane), and infill pattern (line).

2.1 Printing process

The printing was performed using the Ender® printer with extruder nozzle diameter equal to 0.4 mm (Figure 3). For this test, the printing parameter settings were made as presented in Table 2. Applying Equation (3), we have a total of four combinations, resulting in four groups of test specimens with all possible variations. According to the ASTM D638 standard, for each parameter configuration, 5 samples must be printed, resulting in the printing of 20 specimens. For this study, processing temperatures (extrusion) of 215ºC and 60ºC for the build plate were used.

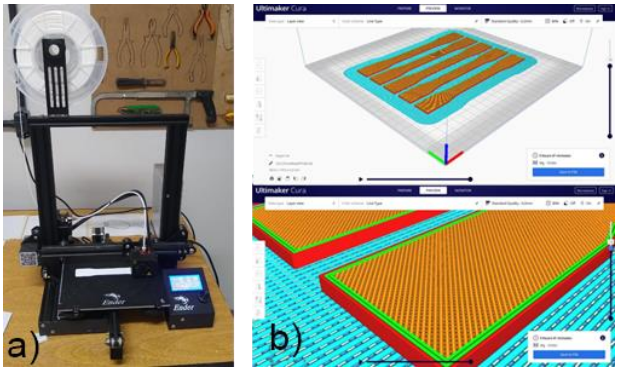

Figure 3. ENDER® 3D printer (a), Ultimaker Cura 3D® slicing software (b). Source: Author (2023).

Table 2. Experimental matrix for specimen printing.

Configuration	Extruder nozzle speed (mm/s)	Infill percentage (%)
C1	90	80
C2	50	80
C3	90	50
C4	50	50

It is believed that higher working speeds may result in specimens with an inferior finish and may influence adhesion between the printed layers. The filling percentage is directly related to the percentage of voids in the cross-sectional area of the specimen and consequently influences the mechanical resistance. Therefore, for this initial phase of the work, these printing parameters were selected for study.

The 3D printing process is essentially divided into five stages: (1) modeling, (2) conversion, (3) slicing, (4) printing, and (5) finishing. The modeling stage involves creating the geometry of a three-dimensional model. This model can be generated using computer-aided design (CAD) software. In this project, SolidWorks® software was used, and the geometry was based on a standard, as previously mentioned. During the conversion phase, the data obtained in CAD was converted to the STL (Surface Tessellation Language) format, which captures the information of each surface of the 3D model in the form of triangular sections, where the spatial coordinates of the vertices are defined and transmitted to the printer for object fabrication.

Next, in the third stage, the printer software performed the slicing of the file, generating the G-code. Ultimaker Cura 3D® software, version 4.5, was used for this purpose. During the slicing process, the printing parameters were inputted, as mentioned earlier. Subsequently, the G-code was sent to the printer using an SD card to print consecutive layers of the designated material.

The printing process carried out on the Ender® machine requires attention to the leveling of the print bed, as it is done manually and should be at a distance that allows the extruder nozzle to move freely on the bed without exerting pressure. Therefore, three samples were printed for a preliminary test of the printing parameters and adjustments to the testing machine.

One sample from the preliminary test showed warping and was discarded due to this factor. After this, other preliminary printing tests were carried out using adhesive spray on the table. It was observed that the spray solved the warping problem and the method was adopted for the definitive impression. At the end of the preliminary test prints, small grooves were observed on the sides of the samples (Figure 4). These grooves remained in the same location in all samples, as they correspond to the start and end points of each layer, leaving a marking in the vertical direction.

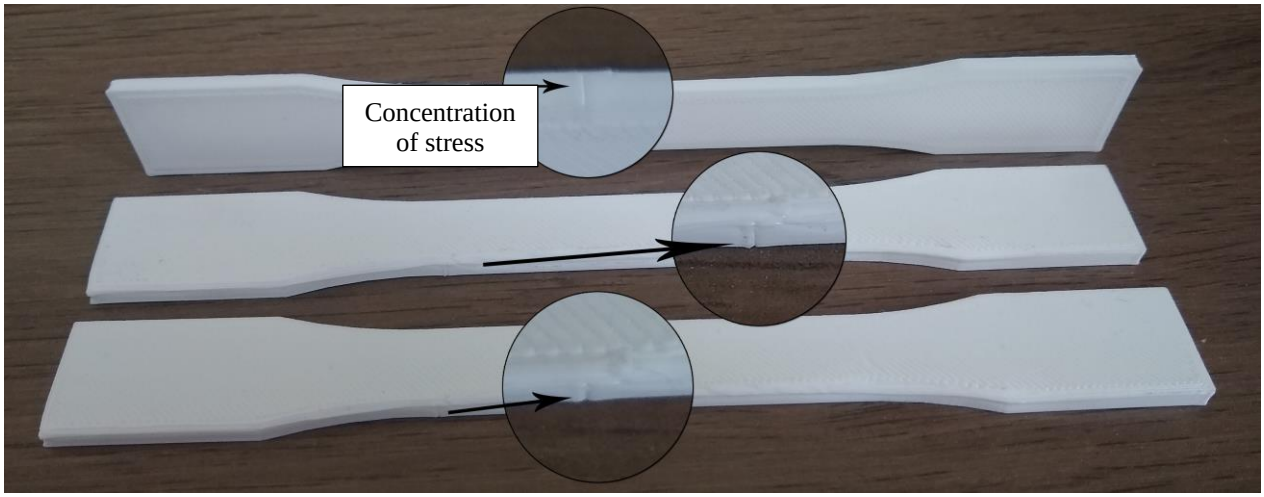

Figure 4. White PLA test specimens with side grooves for preliminary testing. Source: Author (2023).

The addition of the raft parameter was applied to all final sample groups during the slicing phase in order to improve the adhesion of the initial layer of the part and reduce the effect of these side grooves. The raft serves as a sacrificial primary surface (Figure 5) that enhances the adhesion of the first layer to the print bed.

However, the use of the raft did not eliminate the appearance of the side grooves in the test specimens. Starting the print layer in the same location consistently creates a concentration of stress, resulting in the formation of these marks. It is worth noting that the marks were significantly reduced with the use of the raft. This marks can eliminate change the initial printer configuration.

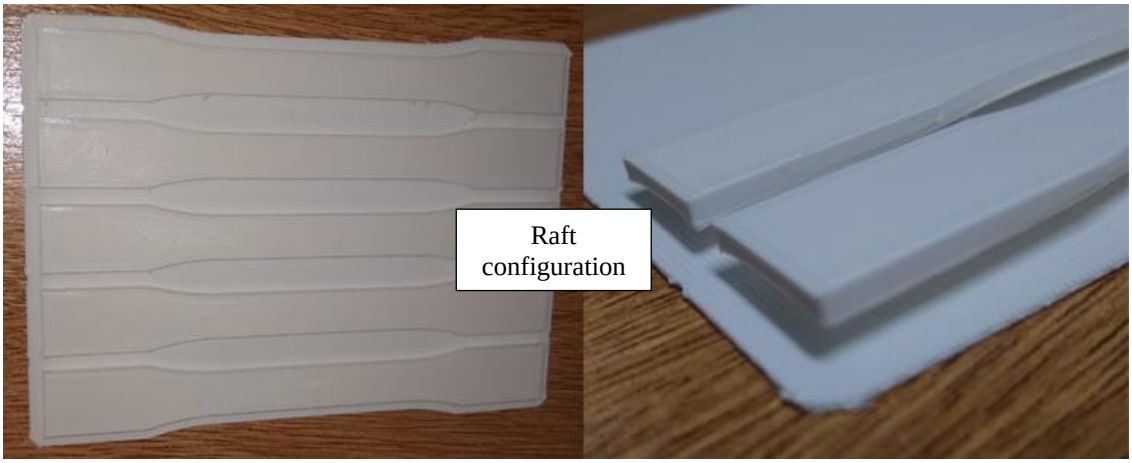

Figure 5. Printing of a set of samples with the raft configuration. Source: Author (2023).

2.2 Tensile test

The tensile test was conducted at the Department of Agricultural Engineering of the Universidade Federal de Viçosa (UFV), in the Agricultural Mechanization Laboratory (LMA). The tested specimens followed the dimensions and methods defined by ASTM D638 standard. The universal testing machine, Instrom 3365®, with a 5 kN load cell, was used, and the testing speed, according to the standard, was set at 5 mm/min. At the end of the test, the machine provides data on force, displacement, stress, and time.

In each sample, the width and thickness were measured in the deformation section, following with a maximum variation of 0.2 mm in the dimensions of the printed specimens compared to the standard requirements. All specifications and measurements of the specimen were entered into the machine's software. The specimens were placed in the grips of the testing machine, aligning the long axis of the sample with the grips, with an imaginary line connecting the grip fixation points to the machine. The distance between the ends of the gripping surfaces was 115 mm, as indicated in Table 1. The grips were tightened uniformly and firmly to prevent the samples from slipping during the test but not to the point of crushing the sample. After tightening, the extension and force were zeroed in the machine's software, and all conditions were ready to start the test. After the test was completed, the fractured specimen was removed, and all the previous steps were repeated for the remaining samples.

The tensile test provides force and displacement values. The machine's software records pairs of these values for numerous points during the test. With these values, all the desired results can be calculated such as tensile strength (S_{ut}) and modulus of elasticity (E). Knowing the maximum force value and the nominal cross-sectional area of the specimen, the maximum stress can be calculated using the maximum stress equation. With the maximum displacement value and the initial length of the test zone, the maximum strain can be approximately calculated using the strain equation.

2.3 Experimental design and statistical analysis

An experiment was conducted with variations in the extruder nozzle speed and infill percentage, as shown in Table 2. The experiment used a completely randomized design in a 2 x 2 factorial scheme (extruder nozzle speeds x infill percentages), with five replications each, resulting in a total of 20 experimental units. The effect of the extruder nozzle speed and infill percentage on tensile strength and modulus of elasticity was studied. A variance analysis was performed for each experiment, evaluating all input factors together (extruder nozzle speed and infill percentage).

Both ultimate tensile strength and modulus of elasticity were studied using regression analysis, considering the factors of extruder nozzle speed and infill percentage. The fitted models were chosen based on the significance of the estimated parameters, determined through the t-test. The coefficient of determination for each fitted model was presented. A significance level of 5% was set for all analyses, considering that, as mechanical properties, there would not be high variability. All statistical analyses were performed using the Minitab® software and the surfaces were plotted using Matlab®.

3. RESULTS AND DISCUSSIONS

3.1 Mechanical analysis

In the experiment, four combinations were tested with two infill percentages (80% and 50%) and two nozzle speeds (90 and 50 mm/s). Table 3 shows the average values and standard deviations of the maximum extension, maximum load, tensile strength, maximum deformation, and modulus of elasticity for each configuration tested in the tensile test.

Table 3. Results obtained in the tensile test.

Average Data					
Configuration*	**Maximum Extension (mm)**	**Maximum Load (N)**	**Tensile Strength (MPa)**	**Maximum Deformation (mm/mm)**	**Modulus of Elasticity (MPa)**
C1	2,35±0,136	1219±32,8	36,6±0,99	0,0413±2,3E-3	889,9±42,5
C2	2,44±0,134	1265±42,4	38,0±1,28	0,0428±2,4E-3	887,4±19,8
C3	2,55±0,046	1136±12,1	34,1±0,36	0,0447±8,2E-4	764,4±21,7
C4	2,36±0,101	1170±30,2	35,1±0,91	0,0415±1,8E-3	848,0±24,8

*Configuration: Nozzle speed(mm/s) e infill percentage (%); C1=90 e 80; C2=50 e 80; C3=90 e 50; C4=50 e 50.

According to the results obtained in the analysis of variance (Table 4), there was no significant influence of the parameters for the interaction between speed and infill percentage on the ultimate stress factor ($P>0.05$), only an individual influence of the infill percentage. On the other hand, in Table 5, it can be observed that the interaction of the variation sources is significant for the modulus of elasticity factor ($P<0.05$).

Table 4. Analysis of variance results for the influence of printing parameters on Ultimate Stress (S_{ut}).

Tensile Strength (MPa)					
Source of Variation	**Degrees of freedom**	**Sum of squares**	**Mean square**	**F**	**Value-P**
V	1	3,200	3,200	4,414	0,0519
P	1	24,20	24,20	33,379	0,0000
V*P	1	0,200	0,200	0,276	0,6066
Error	16	11,60	0,7250		
Total	19	39,20			

**significant at the 5% probability level, cv (%) = 3,02

Table 5. Analysis of variance results for the influence of printing parameters on Elastic Modulus (E).

Modulus of Elasticity (MPa)					
Source of Variation	**Degrees of freedom**	**Sum of squares**	**Mean square**	**F**	**Value-P**
V	1	5281,25	5281,25	9,844	0,0064
P	1	21714,05	21714,05	40,474	0,0000
V*P	1	5951,25	5951,25	11,093	0,0042
Error	16	8584,00	536,50		
Total	19	41530,55			

** significant at the 5% probability level, cv (%) = 3,42

The infill percentage was the variable with a significant effect on S_{ut}, as indicated by the adjusted parameter presented in Table 6, and the representative curve is shown in Figure 6. It can be observed that the maximum estimated values for the S_{ut} are achieved with an 80% infill percentage.

Table 6. Results of the t-test for the adjusted parameters of the model used for Ultimate Tensile Strength (Sut).

Tensile Strength (MPa)					
Variable	**Degrees of freedom**	**Estimated parameters**	**Standard error**	**t value**	**P value**
Intercept	1	24,14833	0,86885	27,79	0,000
P	1	0,07133	0,01302	5,480	0,000

**significant at a 5% level

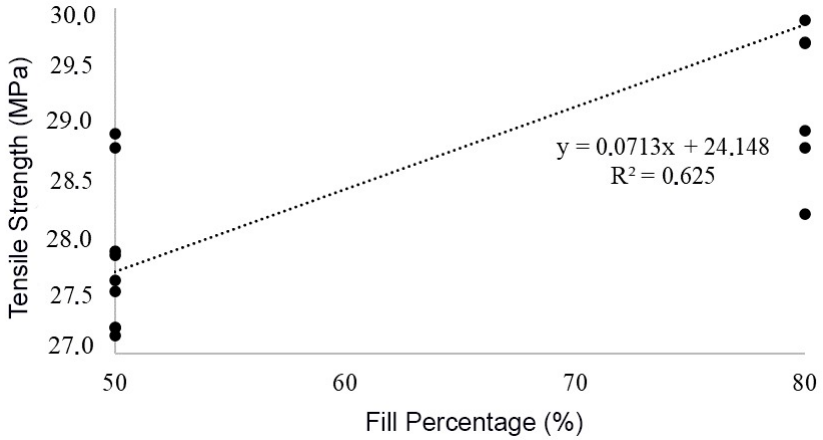

Figure 6. Variation of Tensile Strength (S_{ut}) as a function of filling percentages (50 and 80%).

In Table 7, the result for the regression analysis for E is presented. It is possible to observe a different behavior compared to Sut, as the interaction of the parameters is statistically significant for the modulus of elasticity.

Table 7. Results of the analysis of variance for the adjusted model of Modulus of Elasticity (E).

Modulus of Elasticity (MPa)					
Source of Variation	**Degrees of freedom**	**Sum of squares**	**Mean square**	**F**	**Value-P**
Regression	3	33012	11003,9	20,53	0,000
V	1	8343	8343,0	15,56	0,001
P	1	1116	1116,1	2,08	0,168
V*P	1	5915	5914,7	11,03	0,004
Error	16	8576	536,0		
Total	19	41588			

** significant at the 5% probability level, CV (%) = 3,41, R^2=79,38%

In Table 8, the results of the t-test for the estimated parameters are presented, concerning the adjusted model to represent the interaction of the printing parameters on the E. The coefficient of determination for the adjusted model was 79.38%, indicating that a large portion of the data is explained by the fitted equation. It can be observed that the behavior of the E followed the same trend as S_{ut}, with maximum values concentrated at the 80% filling percentage. However, this time it interacted with a printing speed of 90 mm/s, as shown in Figure 7. This result is plausible, as having more material in the part would generally lead to increased mechanical properties. Regarding the printing speed, it seems that it did not have a significant influence on the loss of specimen characteristics, possibly due to the small size of the part.

Table 8. Results of the t-test for the adjusted parameters of the model used for the Modulus of Elasticity (E).

Modulus of Elasticity (MPa)					
Variable	Degrees of freedom	Estimated parameters	Standard error	t value	P value
Intercept	1	853,14367	83,80560	10,18	0,000
V	1	-4,54157	1,15116	-3,95	0,001
P	1	-1,81283	1,25630	-1,44	0,168
V*P	1	0,05732	0,01726	3,32	0,004

**significant at a 5% level, V – extruder nozzle speed; P – infill percentage

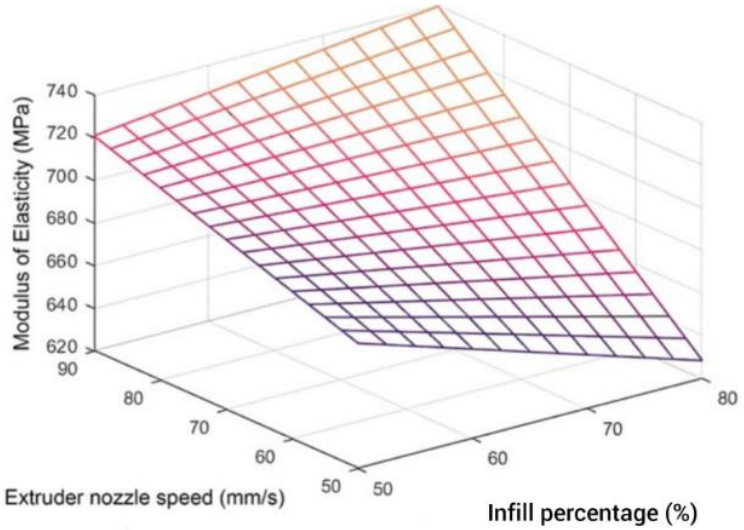

Figure 7. Adjusted response surface representing the modulus of elasticity (E = 853,1 – 4,54V – 1,81P + 0,0573V*P).

4. CONCLUSIONS

Based on the data and discussions presented in this study, it can be observed that there is a direct association between the working polymer and the characteristics obtained in the final part. The mechanical strength increased with an increase in the infill percentage and with an extruder nozzle speed. In this case, increasing the infill percentage of the part resulted in stronger and more robust pieces. However, for 3D printing in large-scale production, it is more advantageous to use a smaller mesh of a stronger polymer rather than a robust mesh of a less strong polymer. Therefore, for applications requiring mechanical strength, PLA is recommended for parts subjected to tensile forces.

5. ACKNOWLEDGEMENTS

We thank the Department of Agricultural Engineering of the Universidade Federal de Viçosa, in special the Agricultural Mechanization Laboratory (LMA), for providing the lab equipment used to make the mechanical tests.

6. REFERENCES

Alaimo, G., Marconi, S., Costato, L. and Auricchio, F. Influence of meso-structure and chemical composition on FDM 3D-printed parts, 2017, Composites Part B: Engineering, Vol.6, pp. 371-380.

ASTM, 2014, Standard tests method for tensile properties of plastics. United States: ASTM International.

Bellini, A., Guerrieri, R. and Redaelli, A., 2017, Additive manufacturing of PLA-based materials for tissue engineering applications: a review. Applied Sciences, Vol.7(9), pp. 870.

Fico, D., Rizzo, D., Casciaro, R. and Corcione, C. E., 2022, A review of polymer-based materials for fused filament fabrication (FFF): focus on sustainability and recycled materials, Polymers, Vol. 14(3), pp. 465.

Gibson, I., Rosen, D. W. and Stucker, B., 2015, *Additive manufacturing technologies: 3D printing, rapid prototyping, and direct digital manufacturing*. Springer.

Johnson, A., Smith, B. and Oliveira, C., 2020, Mechanical properties of 3D-printed materials. Journal of Materials Science, Vol. 55(17), pp. 6985-7005.

Mensah, R. A., Edström, D. A., Lundberg, O., Shanmugam, V., Jiang, L., Qiang, X., Försth, M., Sas, G., Hedenqvist, M., Das, O. (2022). The effect of infill density on the fire properties of polylactic acid 3D printed parts: A short communication. Polymer Testing, Vol. 111, pp. 107594.

Rodriguez, J. F., Thomas, J. P. and Renauld, J. E., 2000, Characterization of the mesostructure of fused-deposition acrylonitrile-butadiene-styrene materials. Rapid Prototyping Journal, Vol. 6(3), pp. 175-185.

Santana, L., Alves, J. L., Sabino Netto, A. C. and Merlini, C., 2018, Estudo comparativo entre PETG e PLA para Impressão 3D através de caracterização térmica, química e mecânica. Revista Matéria, Vol.23(4), pp. 12267.

Smith, B., Souza, L., & Pereira, R., 2018, Understanding the mechanical properties of 3D-printed materials: A review. Journal of Manufacturing Processes, Vol. 35, pp. 105-124.

Souza, L., Pereira, R. and Johnson, A., 2019, Materials and mechanical properties of 3D-printed objects. Materials Today Communications, Vol. 20, pp. 100556.

7. RESPONSIBILITY NOTICE

The authors are the only responsible for the printed material included in this paper.